Universal Journal of Environmental Research and Technology
 eISSN 2249 0256
Available Online at: www.environmentaljournal.org
Volume 1, Issue 4: 486-499

Open Access **Research Article**

Predicting Iron Adsorption Capacity and Thermodynamics onto Calcareous Soil from Aqueous Solution by Linear Regression and Neural Network Modeling

[1]Bhaumik R., [1]*Mondal N. K., [1]Das B., [1]Roy P. and [1]Pal K. C.

[1]Department of Environmental Science, The University of Burdwan, Burdwan-713104, W.B, India.

[1]*Corresponding author: nabakumar_mondal@indiatimes.com

Abstract:

Calcareous soil with various physical parameters along with morphological characteristics Fourier Transform Infrared (FTIR), X-Ray Diffraction (XRD) and Scanning Electron microscopy (SEM) was used for removal of Fe^{+2} from aqueous solution through batch process. During batch study various parameters effects on the adsorption capacity of Fe^{+2}. This adsorption was followed by pseudo-second-order kinetic and Langmuir isotherm model. The activation energy was determined at 9.47 kJ/mol indicating physical adsorption. According to D-R model, E_s also supports this. Gibb's free energy (ΔG^0), explains the spontaneous nature of adsorption and negative value of ΔH^0 implies exothermic nature. A six layered feed forward neural network with back propagation training algorithm was developed using twenty one experimental data sets obtained from laboratory batch study. The ANN predicted results were compared with the experimental results of the laboratory test. It was concluded that calcareous soil is an effective adsorbent for removal of Fe^{+2} from aqueous solution.

Keywords: ANN model, Batch adsorption, statistically analysis, thermodynamic parameters

1. Introduction:

In the entire phenomena of civilization pollution is an unsought, unexpected and unforeseen consequence. Iron in ground water, major source of potable water above a certain level make the water unusable mainly for aesthetic considerations (Ahamad and Jawed, 2011). It affects staining on laundries, fixtures and tableware etc. (Deviprasad and Abdullah, 2009). Through the effluent of many industries such as basic steel, inorganic chemicals, alkalis, chlorine, fertilizers and petroleum refining iron is usually discharged into the environment (Dean *et al.,* 1972). It may lead to debilitating and life-threatening problems such as diabetes, heart failure and poor growth (Deviprasad and Abdullah, 2009). It also causes conjunctivitis, chloroidities and retinitis if it contacts and remains in the tissue (Atolaiye *et al.,* 2009). According to WHO (1993), the acceptable value of iron in drinking water is 0.3 mg/L. Traditional technologies such as aeration and separation, ion-exchange (Vaaramaa and Lehto, 2003), oxidation with oxidizing agents (Ellis *et al.,* 2000) are most widely used for removal of iron from drinking and groundwater. The adsorption process, proved its advantage over the other process because of its cost effectiveness and the high-quality of the treated effluent it produces (Najim *et al.,* 2009). Different natural materials are used such by previous researchers as peat, sand, ash, leaf powder, eggshell dust (Yeddou and Bensmaili, 2007) for removal of Fe^{+2} ions from contaminated water. Calcareous soil is mainly composed of calcium carbonate and calcium phosphate. In recent years ANN has become a popular choice among engineers and scientists as one of the powerful tools for predicting contamination and concentration of different effluents and chemicals in drinking water, wastewater and aquifers. Various researchers (Meenakhsipriya *et al.,* 2009) used ANN models to predict adsorption efficiency. This study was evaluated the efficiency of calcareous soil in the adsorption of Fe^{+2} from aqueous solution. Through artificial neural network (ANN), we can predict the function of many variables and parameters. In this study, the data obtained from batch experiments were divided into input matrix and desired matrix.

2. Materials and Methods:

2.1 Adsorbent Collection and Preparation:

Calcareous soil sample was collected from Birbhum district, West Bengal, India. Then the sample was grounded in a mortar and sieved as to pass through 150 μm mesh size. The soil sample stored in sterile, closed plastic containers and used as an adsorbent (Figure a).

Figure a: Calcareous soil as in form of both raw materials and modified adsorbent

2.2 Adsorbate Solution Preparation:

Stock solution of Fe^{+2} was prepared (1000 mg/L) by dissolving the desired quantity of ferrous ammonium sulphate salt (analytical grade from Merck, Pvt. Ltd. India) in double distilled water. Experimental adsorbate solutions of different concentrations were prepared from stock solution by proper dilution.

2.3 Batch Study:

Batch adsorption experiments were carried out in a 250 ml stoppered conical flask for removal of Fe^{+2} from the aqueous phase using calcareous soil by using temperature controlled magnetic stirrer (BZMS448 REMI Equipments; Pvt. Ltd. Mumbai, India). The solution pH (2-10), adsorbent dose (1.0-11.0 g/100 ml), stirring rate (40-250 rpm), contact time (20-120 min), initial metal concentration (0.1-15.0 mg/L) and temperature (303-333 K) were varied. The solutions were filtered and the remaining concentrations of Fe^{+2} after adsorption were determined by using UV-Vis spectrophotometer (Systronics, Vis double beem Spectro 1203). Each experiment was conducted three times and average values are reported. To confirm the sorption of Fe^{+2} on the walls of Erlenmeyer flasks was negligible; control experiments were performed without addition of adsorbent. In this study the effect of other co-ions (HCO^-_3, SO^{-2}_4, Cl^-, NO^-_3, Na^+, Mg^{+2}, Ca^{+2}) on adsorption of were also observed. The amount of Fe^{+2} adsorbed at equilibrium, q_e (mg/g) was determined using the flowing equation:

$$q_e = \frac{(C_i - C_e)V}{m} \quad (1)$$

Where, V = Volume (L) of the equilibrated solution

m = Mass of the adsorbent (g)

C_i = Initial concentration of metal ion (mg/L)

C_e = Equilibrium concentration of Fe^{+2} (mg/L)

2.4 Artificial Neural Network (ANN):

A neural network is a massively parallel distributed processor made up of simple processing units, which has a natural propensity for storing experimental knowledge and making it available for use. Neural Network Toolbox Neuro Solution 5 ® mathematical software was used to determine Fe^{+2} adsorption efficiency. The standardized back-propagation algorithm was used for the training of three ANN models viz. tan1.5h, sigmoid1 and tan h. These trained ANN models were then tested and validated with the experimental results to estimate the Fe^{+2} concentrations (Figure b).

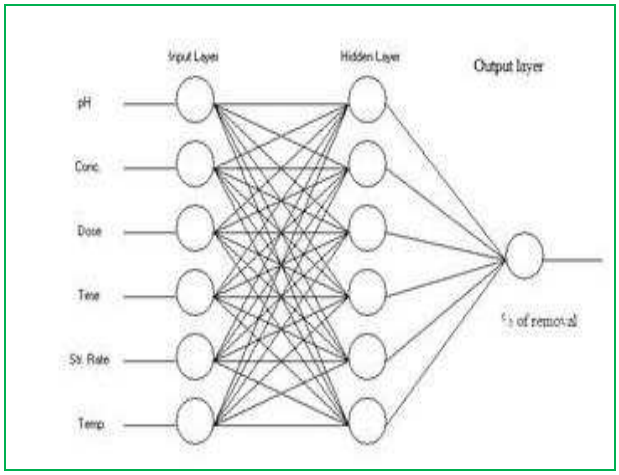

Figure b: Neural Network Architecture

3. Results and Discussions:

3.1 Characterization of Adsorbent:

The physical and chemical properties of calcareous soil sample are presented in Table 1. Soil sample contains high surface area which is

directly responsible for better adsorption (Table 1). Zero point charge curve (Figure c) shows p^H of the solution affects the surface charge of calcareous soil as well as the degree of ionization and the surface is active for adsorption of Fe^{+2} at higher pH (than zero point) due to deposition of OH^- ions. The zero point change of calcareous soil was determined by the solid addition method (Mondal, 2010).

Table 1: Characteristics of the calcareous soil used in this study

Parameters	Values
pH	6.59±0.16
Electrical conductivity (mS/m)	2±0.55
Specific gravity	0.846±0.01
Moisture content (%)	1.17±0.03
Bulk density (g/cm^3)	0.802±0.01
Particle density (g/cm^3)	1.075±0.6
Porosity (%)	25.4±3.08
Cation exchange capacity (mequiv./100g soil)	36±2.64
Na^+ (mg/L)	12.2±2.69
K^+ (mg/L)	45.95±0.63
Ca^{+2} (meq/100g)	6±0.08
Mg^{+2} (meq/100g)	4±0.32
Particle size (μm) (determined by Geosyn Test Sieve)	150±9.86
BET Surface area (m^2/g) (estimated by Quantachrome surface area analyzer (model- NOVA 2200C	21.2±2.85

3.2 Evidences for Adsorption:

The IR spectra of the calcareous soil before and after adsorption of Fe^{+2} have shown in Figure d (before and after). The peaks of calcareous soil was observed (Figure d) at 3448.34, 2926.85 and 2850.55 cm^{-1} which refers to group (-OH), identical alkyl group (-CH_2) and aldehyde group (-CHO) respectively. Also the clear band at 1628.89 and 402.18 cm^{-1} were to be the presence of (C=C) and C-O, respectively (Stewart, 1997). The surface IR characterization of calcareous soil indicated the presence of many functional groups which were able to bind with the iron metal. This clearly indicates the adsorption of metal ion on the adsorbent by physical force not by chemical combination.

The XRD diagrams of calcareous soil and metal ions adsorbed soil have shown in Figure e (before and after). The intense main peak shows the presence of highly organized crystalline structure of calcareous soil (Renmin *et al.,* 2005). After the adsorption of Fe^{+2}, the intensity of highly organized peaks is slightly diminished. This has attributed to the adsorption of metal ions on the upper layer of the crystalline structure of the calcareous soil surface by means of physisorption.

The SEM images of calcareous soil before and after metal ions-adsorbed calcareous soil have been shown in Figure f (before and after). The bright spots show the presence of tiny holes on the crystalline structure of calcareous soil, after treatment of metal ions the bright spots became black shows the adsorption of the metal ions on the surface of the calcareous soil.

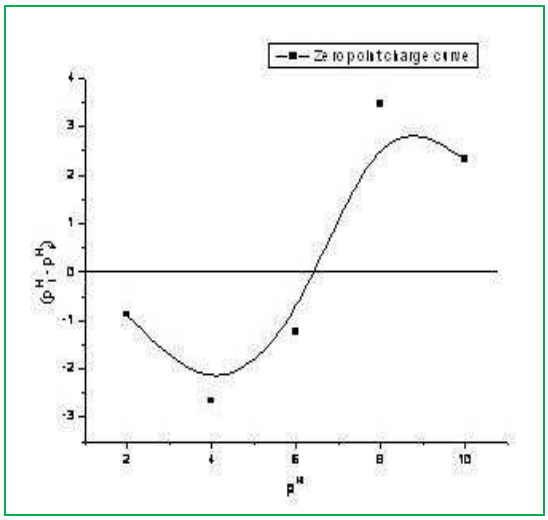

Figure c: Zero point charge of calcareous soil (experimental conditions: adsorbent dose: 1.5 g/100 ml, temperature: 303K)

3.3 Effect of p^H:

P^H of the solution is an important controlling parameter in adsorption process (Wasewar *et al.,* 2009). Figure g shows the maximum removal of Fe^{+2} at p^H of 7.0. At lower p^H values, the H^+ ions compete with metal cations for exchange sites in the system and decrease in adsorption at higher p^H was due to the formation of soluble hydroxy complexes (Wasewar *et al.,* 2009). Similar observation has been reported for sorption of iron onto activated carbon prepared from plant materials (Karthikeyan and Sivailango, 2008).

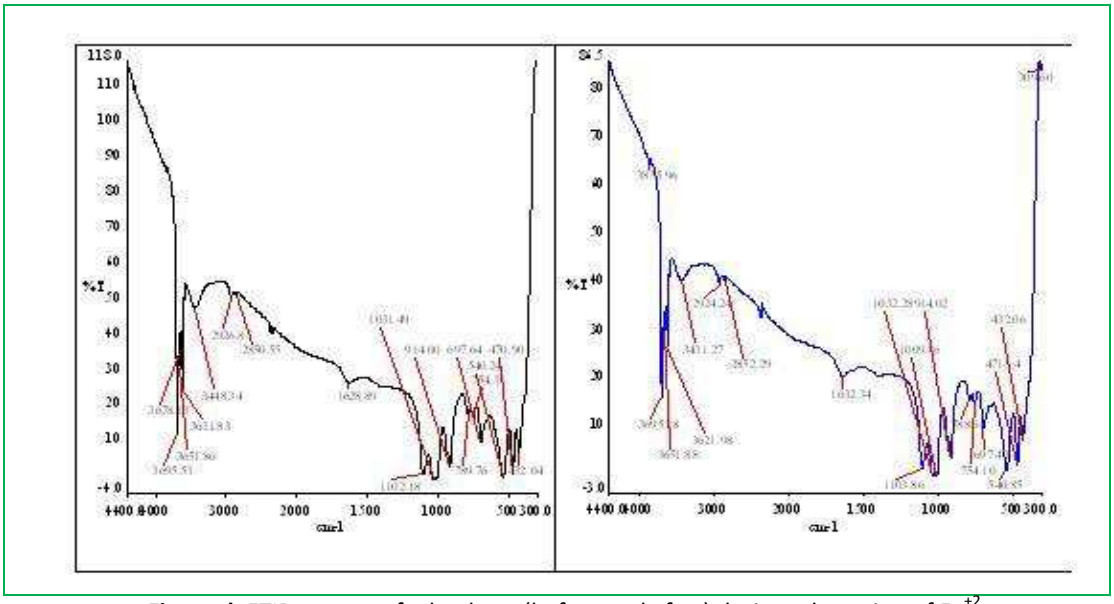

Figure d: FTIR spectra of adsorbent (before and after) during adsorption of Fe^{+2}

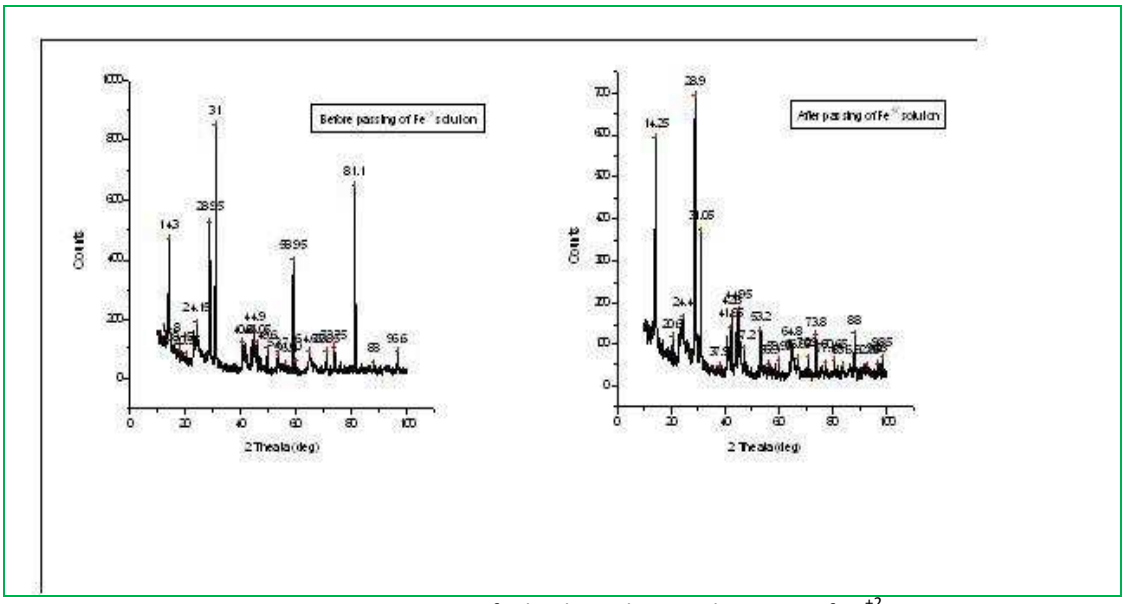

Figure e: XRD spectra of adsorbent during adsorption of Fe^{+2}

3.4 Effect of Adsorbent Dose:

The effect of calcareous soil dose for removal of Fe^{+2} from 6.0 mg/L of metal solution at a temperature 303 K for contact time of 60 min is shown in Figure h. It can be observed that the percent of adsorption increases with adsorbent dose from 1.0 to 11.0 g/100 ml solution. Increase in adsorption with adsorbent dose can be attributed to increased adsorbent surface area and availability of more adsorption sites. A similar trend has been reported for adsorption of Fe^{+2} onto activated carbon from *Zea maize* (Arivoli *et al.,* 2011). The optimum value of adsorbent dose was found to be 5.0 g /100 ml of solution and was used for the later experiments.

3.5 Effect of Stirring Rate:

The effect of different stirring rate were conducted by varying speeds from 40-250 rpm, at optimum pH of 7.0 with adsorbent (calcareous soil) dose of 5.0 g/100ml and contact time of 60 min (Figure i). The percentage adsorption is less at lower stirring rate and increases with the stirring rate up to 200 rpm and thereafter remains more or less constant. The reason for the increase in efficiency is that at higher speeds better contact between the adsorbent and adsorbate is possible (Tembhurkar and Dongre, 2006).

3.6 Effect of Contact Time:

Contact time between the Fe^{+2} and the adsorbent is of significant importance in adsorption process. The contact time curve (Figure j) shows that removal was very rapid in the first 60 min, then the adsorption slowly increased and removal reached equilibrium at 100 min. It also reveals that the curves are smooth and continuous, leading to saturation, suggesting the possible monolayer coverage of Fe^{+2} ions on calcareous soil surface (Najim *et al.,* 2009). Similar findings have been reported by other investigators (Najim *et al.,* 2009; Arivoli *et al.,* 2011; Moreno *et al.,* 2010).

3.7 Effect of initial concentration of Fe^{+2} :

For a given mass of adsorbent, fixed amount of adsorbate can be adsorbed. So the initial concentration of adsorbate solution is very important. The effect of different initial Fe^{+2} concentrations on the adsorption is presented in Figure k. The percentage removal of Fe^{+2} decreased with increasing initial concentrations and showed little decrease at higher concentrations, but the actual amount of Fe^{+2} adsorbed per unit mass of adsorbent increased with increase in initial concentration in test solution. This was because of the decrease in resistance for the uptake of solute from solution with increase in metal concentration (Wasware *et al.,* 2009). Similar results were reported for adsorption of Fe^{+2} from aqueous solution onto Zea maise dust (Arivoli *et al.,* 2011).

3.8 Effect of Temperature:

Temperature is an additional factor, which influence greatly any adsorption process. Batch adsorption experiments were carried out at different temperatures ranging from (303-333 K). Figure l displays the percent removal of Fe^{+2} decreased with increasing temperature. This was due to weakening of the physical bonds between the adsorbate molecules and the active site of the adsorbent (Chowdhury and Saha, 2010).

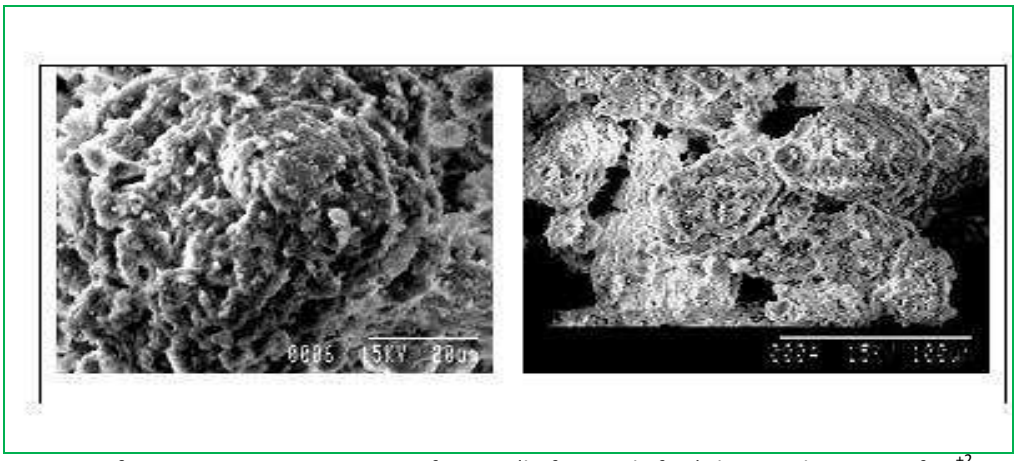

Figure f: SEM images at 20µm magnification (before and after) during adsorption of Fe^{+2}

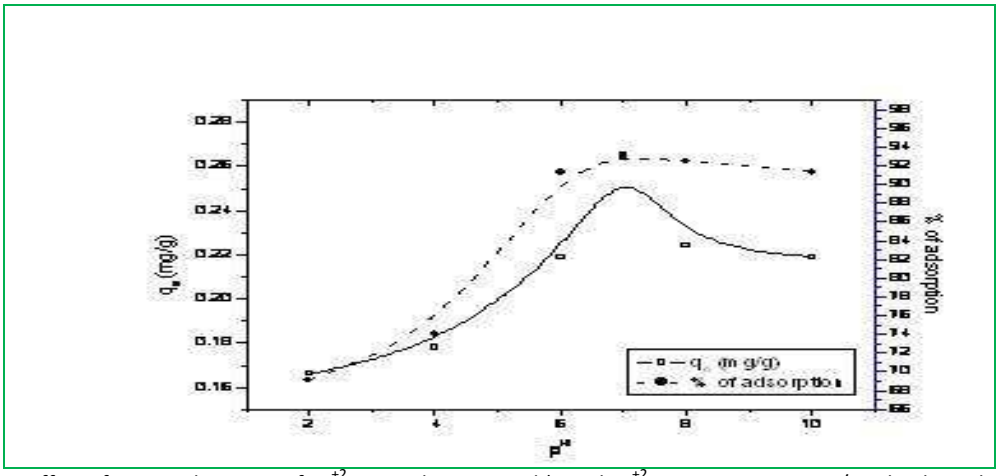

Figure g: Effect of pH on adsorption of Fe^{+2} onto calcareous soil (Initial Fe^{+2} concentration: 6 mg/L, adsorbent dose: 0.5 g/100 ml of solution, contact time: 60 min, stirring rate: 120 rpm, temperature: 303 K)

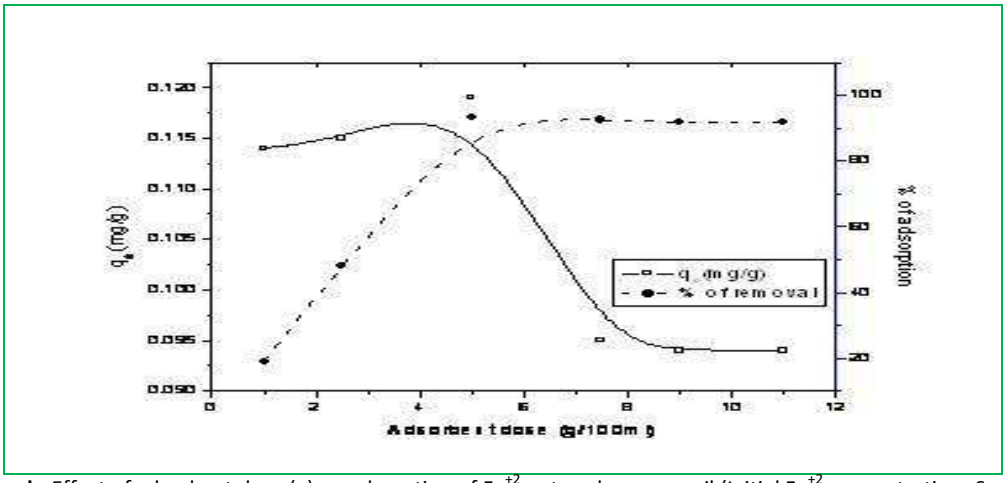

Figure h: Effect of adsorbent dose (g) on adsorption of Fe^{+2} onto calcareous soil (Initial Fe^{+2} concentration: 6 mg/L, pH: 7.0, contact time: 60 min, stirring rate: 120 rpm, temperature: 303 K)

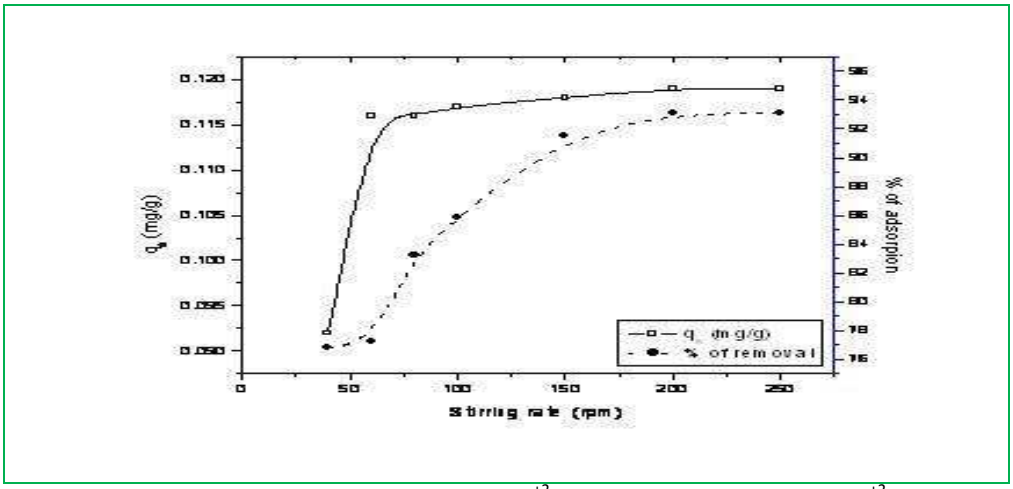

Figure i: Effect of stirring rate (rpm) on adsorption of Fe^{+2} onto calcareous soil (Initial Fe^{+2} concentration: 6 mg/L, pH: 7.0, adsorbent dose: 5.0 g/100ml, contact time: 60 min, temperature: 303K)

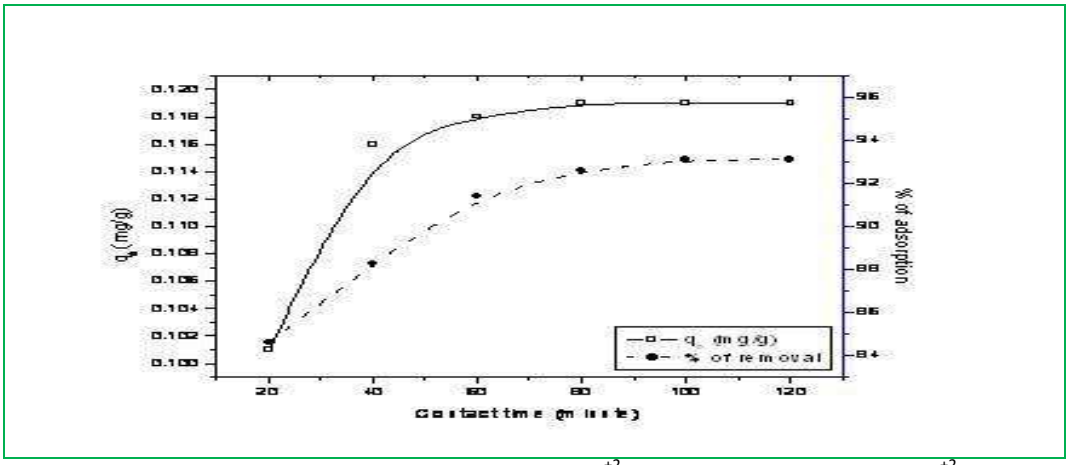

Figure j: Effect of contact time (min) on adsorption of Fe^{+2} onto calcareous soil (Initial Fe^{+2} concentration: 6 mg/L, pH: 7.0, adsorbent dose: 5.0 g/100ml, stirring rate: 200 rpm, temperature: 303K)

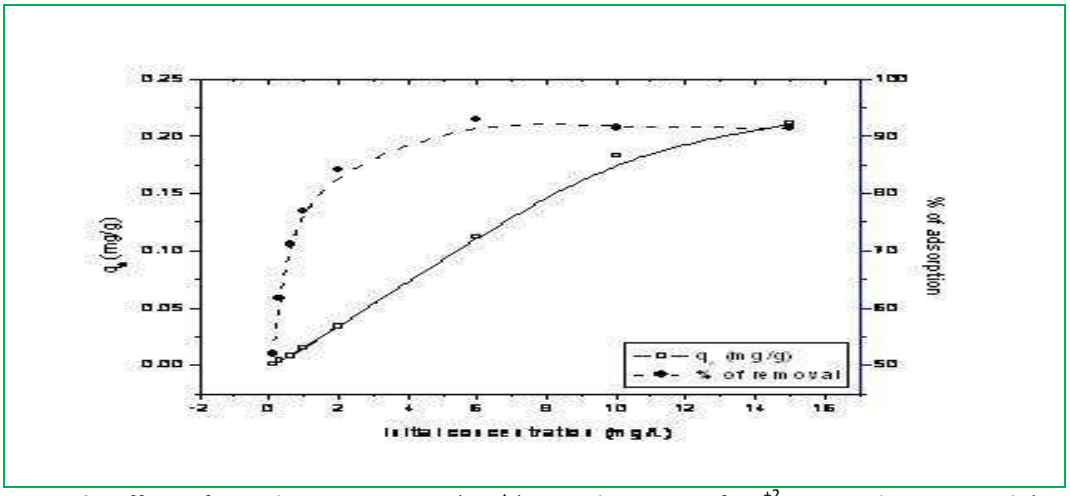

Figure k: Effect of initial concentration (mg/L) on adsorption of Fe^{+2} onto calcareous soil (pH: 7.0, adsorbent dose: 5.0 g/100ml, stirring rate: 200 rpm, contact time: 100 min, temperature: 303K)

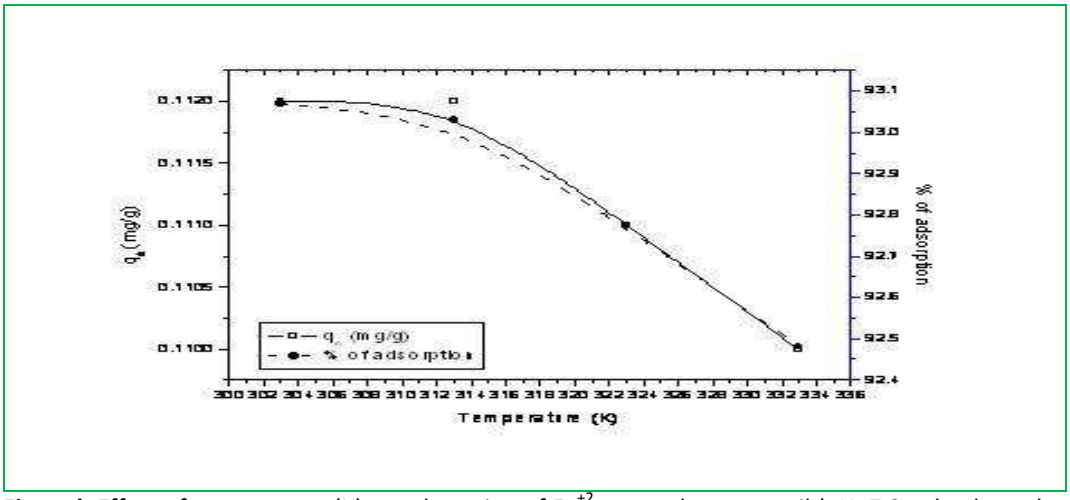

Figure l: Effect of temperature (K) on adsorption of Fe^{+2} onto calcareous soil (pH: 7.0, adsorbent dose: 5.0 g/100ml, stirring rate: 200 rpm, contact time: 100 min, initial concentration: 6.0 mg/L)

3.9 Kinetic Study:

Three kinetic models, pseudo-first-order, pseudo-second-order and intra-particle diffusion were used (equations are shown in Table 2) to find out the best fit rate of reaction for the adsorption of Fe^{+2} ions onto calcareous soil. Based on linear regression correlation coefficients, calculated q_e values and error functions (SSE, SAE, X^2, AIC, % of Error and r^2) (Table 3 and Table 4) the rate of adsorption reaction follows the pseudo-second-order kinetic model. Kinetic results were also presented in the form of the pseudo-second order kinetic model in Table 3 at different concentrations of Fe^{+2}. To identify the diffusion mechanism, the kinetic results were analyzed using the intra-particle diffusion model (Webber-Morris Model)(Webber and Morris, 1963). According to this model, the plot of q_e versus the square root of time should be linear if intra-particle diffusion model is involved in the adsorption process and intra-particle diffusion is the rate controlling step (Oladoja *et al.,* 2008). But present study shows that the plots do not pass through the origin, this indicates some degree of boundary layer control and further shows that intra-particle diffusion is not the only rate-controlling step (Table 3).

Table 2: Equations of kinetic models and error function

Parameters		Linear form	References	plot	Parameters
Kinetic models	Pseudo-first-order	$\log (q_e - q_t) = \log q_e - \frac{k_1 t}{2.303}$	(Theivarasu *et al.,* 2011)	log (q_e-q_t) vs. t	q_e = intercept, k_1 = (slope x 2.303)
	Pseudo-second-order	$\frac{t}{q_t} = \frac{1}{k_2 q_e^2} + \frac{t}{q_e}$		t/q_t vs. t	q_e = 1/intercept, k_2 = intercept^2 / slope , h = 1/slope
	Intra particle diffusion model	$q = k_{id} t^{½} + C$		q vs. $t^{1/2}$	k_{id} = slope C=intercept
Error equations	sum of the square of the errors (SSE)	$SSE = {}^{n}\sum_{i=1} (q_{e\,estm} - q_{e\,exp})_i^{2}$		(Wasewar et al., 2009)	
	sum of the absolute errors (SAE	$SAE = n \sum_{i=1} \lvert q_{e\,estm} - q_{e\,exp} \rvert_i$			
	Chi-square (X^2)	X^2 given as = $n \sum_{i=1} (q_e - q_{em})^2 / q_{em}$			

Table 3: Pseudo-first and second-order kinetic, intraparticle diffusion parameters on adsorption of Fe^{+2} onto calcareous soil by using linear methods

Conc. (mg/L)	Pseudo-first-order			Pseudo-second-order				Intra-particle diffusion		
	K_1	q_e (mg/g)	R^2	K_2	q_e (mg/g)	h	R^2	K_{id}	C	R^2
0.6	0.018	0.006	0.283	10.34	0.012	0.001	0.99	0.001	0.007	0.94
6.0	0.031	0.0035	0.663	1.243	0.133	0.02	0.99	0.003	0.083	0.98
15.0	0.041	0.001	0.535	3.98	0.273	0.29	1	0.001	0.259	0.93

Table 4: Error analysis for kinetics models on adsorption of Fe^{+2} onto calcareous soil

Errors	Pseudo-first-order			Pseudo-second-order		
	0.6 (mg/L)	6.0 (mg/L)	15.0 (mg/L)	0.6 (mg/L)	6.0 (mg/L)	15.0 (mg/L)
SSE	0.0001	0.013	0.073	0.001	0.011	4 10-6
SAE	0.01	0.11	0.276	0.0006	0.006	0.002
X^2	0.025	3.85	91.26	0.035	0.001	1.41

Table 5: Equations of Isotherm models

Isotherm models	Linear expression	plot	Parameters	References
Langmuir	$\frac{1}{q_{eq}} = \frac{1}{q_{max} K_L C_e} + \frac{1}{q_{max}}$	$1/q_e$ vs. $1/C_e$	q_{max} = 1/ intercept, K_L = 1/(slope × q_m)	(Langmuir, 1916)
Frreundlich	$\log q_{eq} = \log K_F + \frac{1}{n} \log C_e$	$\log(q_e)$ vs. $\log(C_e)$	K_F = intercept, 1/n = slope	(Freundlich, 1906)
Temkin	$q_e = B \ln K_T + B \ln C_e$	q_e vs. $\ln C_e$	B = slope, K_T = intercept	(Wasewar *et al.,* 2009)
D-R	$\ln q_e = \ln q_m - \beta \varepsilon^2$ $Es = \frac{1}{\sqrt{2\beta}}$	$\ln q_e$ vs. ε^2	β = slope, q_m = intercept	(Kalavathaya *et al.,* 2010)

3.10 Equilibrium Isotherm:

The Langmuir, the Freundlich, the Dubinin-Radushkevich and the Tempkin isotherm models (Table 5) were used to describe the equilibrium adsorption data of Fe^{+2} onto calcareous soil. According to both Table 6 and Figure m, the Langmuir isotherm model showed excellent fit to the experimental data with high correlation coefficients at all temperatures. The maximum Fe^{+2} adsorption capacity of calcareous soil was found to be 2.47 mg/g at 303 K. The constant K_L, represents the affinity between the adsorbent and adsorbate and the values of K_L also showed in decreasing order with temperature (Kalavathy *et al.,* 2010) and indicates a low heat of adsorption (Dogan, 2004; Pandey *et al.,* 1984). The empirical Freundlich model also showed a fairly good fit to the experimental equilibrium data at all temperatures studied (R^2>0.93). The values of K_F from the Freundlich model are an indicator of the adsorption capacity of a given adsorbent (Kalavathy *et al.,* 2010). The adsorption capacity (K_F) decreased with increase in temperature (Table 6) which implies the adsorption process as exothermic in nature (Saha *et al.,* 2010). The n should have values lying in the range of 1-10 for favorable adsorption. According to D-R, the constant β gives an idea about the mean free energy E_s (kJ/mol) of adsorption per mole of the adsorbate when it is transferred to the surface of the solid from infinity in the solution. The value of this parameter can give information about the type of adsorption mechanism. In this study the magnitude of E_s were lower than 8 kJ/mol for all studied temperatures and this is indicating that the present adsorption mechanism was physisorption in nature. The Tempkin isotherm constant values are presented in Table 6. It can be concluded that adsorption of Fe^{+2} onto calcareous soil best fitted to Langmuir isotherm model under the temperature range studied and the result implies that the binding energy on the whole surface of the adsorbent was uniform. It also indicates that Fe^{+2} ions were adsorbed by forming a monolayer. The effectiveness of calcareous soil as an adsorbent for iron adsorption was also compared with other reported adsorbents. The maximum adsorption capacity obtained in this study is comparable with other adsorbents as shown in Table 7.

Table 6: Adsorption isotherm parameters for adsorption of Fe^{+2} onto calcareous soil at different temperatures

Temperature (K)	Langmuir isotherm parameters			Freundlich isotherm parameters			D-R isotherm parameters				Tempkin		
	q_{max}	K_L (Lmg^{-1})_	R^2	K_f (mgg^{-1}) (Lmg^{-1})$^{1/n}$	n	R^2	q_m (mgg^{-1}	K	E_s	R^2	B	K_T	R^2
303	2.47	0.114	0.99	0.243	1.18	0.93	1.11	3.43×10^{-3}	3.72	0.95	0.05	43.82	0.93
313	2.31	0.112	0.99	0.237	1.11	0.93	1.08	3.47×10^{-3}	3.61	0.91	0.05	28.65	0.86
323	2.12	0.110	0.98	0.194	1.09	0.89	1.07	3.68×10^{-3}	3.46	0.89	0.04	15.59	0.86
333	2.01	0.106	0.95	0.125	1.06	0.88	1.05	3.81×10^{-3}	3.22	0.87	0.03	9.57	0.86

Table 7: Comparison of Fe^{+2} adsorption capacity of calcareous soil with other reported low-cost-adsorbents

Adsorbent	q_{max} (mg/g)	Reference
Tamarind bark	11.75	(Deviprasad and Abdullah, 2009)
Potato peel watse	7.87	(Deviprasad and Abdullah, 2009)
Zea maise dust	37.17	(Arivoli *et al.,* 2011)
Cattle manure	1.10	(Jordao *et al.,* 2010)
Bengal gram husk	3.294	(Kumar *et al.,* 2010)
Cow bone charcoal	31.43	(Moreno *et al.,* 2010)
Dried pine fruit dust	4.824	(Najim *et al.,* 2009)
Vitex doniana leaf	0.128	(Atolaiye *et al.,* 2009)
Calcareous soil	2.47	Present study

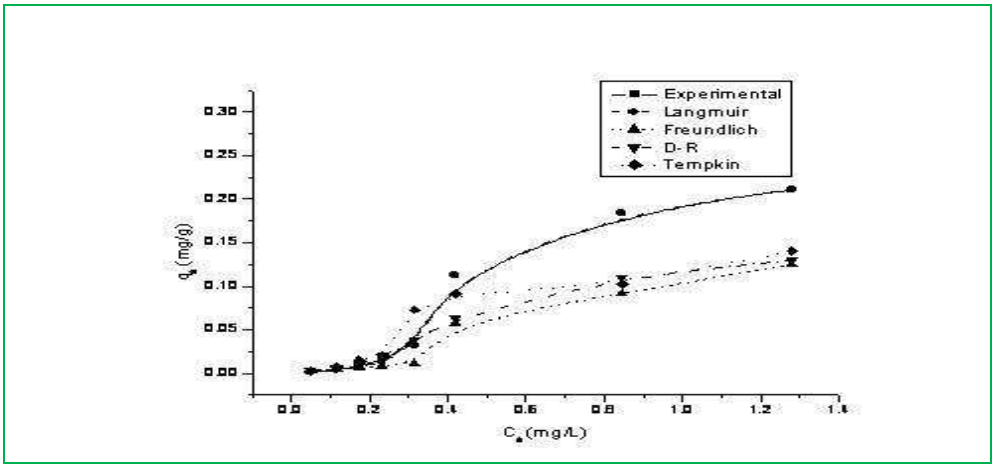

Figure m: Comparison between the measured and modeled isotherm profiles for the adsorption of Fe^{+2} by using calcareous soil on different initial concentration (mg/L): (experimental condition pH: 7.0, adsorbent dose: 5.0 g/100 ml, stirring rate: 200 rpm, contact time: 100 min, temperature: 303K)

3.11 Effects of Co-ions:

The influence of other co-ions such as Cl^-, SO_4^{-2} HCO_3^-, NO_3^-, Ca^{+2}, Na^+, Mg^{+2} which are commonly present in water, on adsorption of Fe^{+2} was also investigated to determine the feasibility of the process for contaminated drinking and groundwater applications. From Figure n, it was observed that at low concentrations of NO_3^-, Cl^-, HCO_3^-, SO_4^{-2}, and Na^+ does not affect of the percentage of adsorption

of Fe^{+2} on calcareous soil, because the interaction of these ions at available sites of adsorbent through competitive adsorption is not so effective. While the concentrations of other ion Ca^{+2} and Mg^{+2} increases, the influence of these ions at available surface sites of the adsorbent through competitive adsorption increase that, decreases the percentage adsorption. The interference was more in the presence of Ca^{+2} and Mg^{+2} ions compared with other ions. This is so because ions with smaller hydrated radii decrease the swelling pressure within the adsorbent and increase the affinity of the sorbent for such ions (Vadivelan and Kumar, 2005). Similar trend was previously reported for adsorption of Fe^{+2} ion onto activated carbon (Arivoli *et al.,* 2011).

3.12 Activation Energy and Thermodynamic Study:

From the pseudo-second-order rate constant k_2 (Table 4.), the activation energy E_a calculated for the adsorption of Fe^{+2} onto calcareous soil was determined using Arrhenius equation (Table 8). By plotting ln k_2 versus 1/T, E_a was obtained from the slope of the linear plot (Figure o) and the value of E_a for Fe^{+2} adsorption onto calcareous soil was 9.47 kJ/mol (Table 9). The activation energy for physical adsorption is usually less than 40 kJ mol^{-1}. In the present study, the value of the activation energy confirms the nature physisorption of Fe^{+2} onto calcareous soil. The result corresponded well with those from the Dubinin-Radushkevich isotherm. The changes of Gibb's free energy (ΔG^0) for the adsorption of Fe^{+2} onto calcareous soil at all temperatures and the value of ΔH^0 and ΔS^0 and are also listed in Table 9. The negative value of $^{\Delta}G^0$ at all temperatures indicates the feasibility of the process and the spontaneous nature of the adsorption onto adsorbent. Decrease in value of $^{\Delta}G^0$ with increase in temperature suggests that lower temperature makes the adsorption easier (Figure p). The negative value of $^{\Delta}H^0$ implies that the adsorption phenomenon is exothermic. The negative value of $^{\Delta}S^0$ suggests that the process is enthalpy driven (Saha *et al.,* 2010).

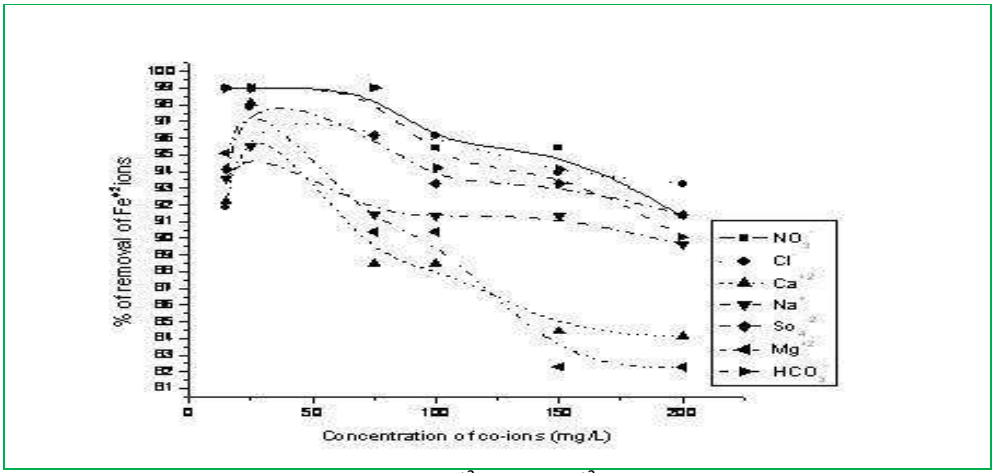

Figure n: Effects of Co-ions on adsorption of Fe^{+2} (Initial Fe^{+2} concentration 6mg/L, pH: 7.0, adsorbent dose: 5.0 g/100ml, stirring rate: 200 rpm, contact time: 100 min, temperature: 303K)

Table 8: Activation energy and Thermodynamic equations

Parameters	Linear Equation	References
Activation energy	$\ln k = \ln A - \frac{E_a}{RT}$	(Lu *et al.,* 2009)
Thermodynamic study	$K_C = \frac{C_{Ae}}{C_e}$ $\Delta G^0 = -RT\ln K_C$ $\log K_C = \frac{\Delta S^0}{2.303R} - \frac{\Delta H^0}{2.303RT}$	(Sujana *et al.,* 2009)

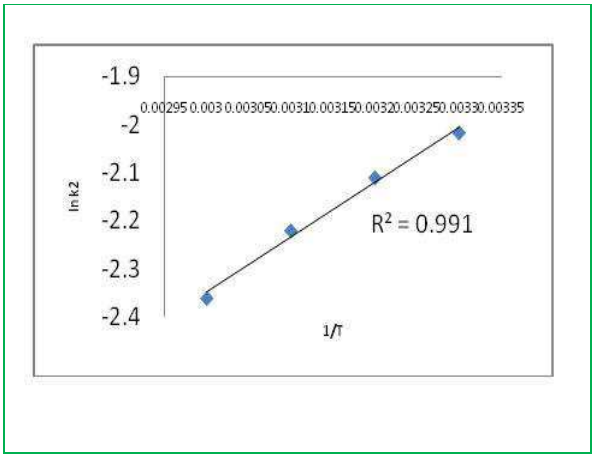

Figure o: Arrhenius equation plot for adsorption of Fe^{+2} onto calcareous soil

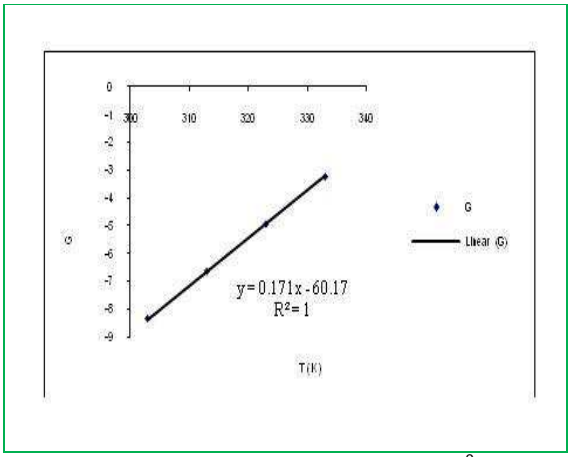

Figure p: Changes of Gibb's free energy (ΔG^0) vs. T (K)

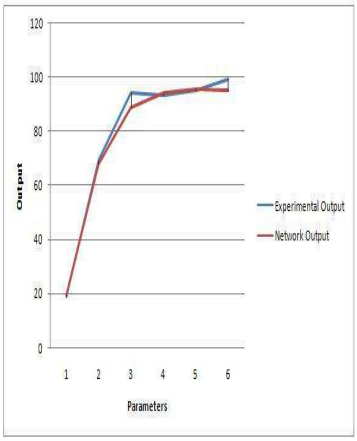

Figure q: Experimental and model output curve tan1.5h

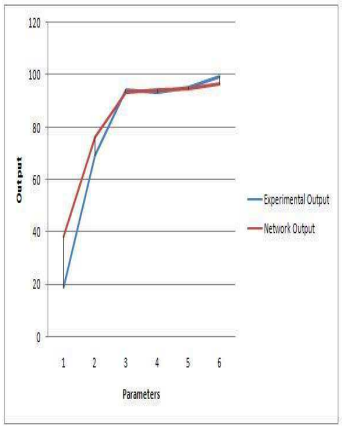

Figure r: Experimental and network output sigmoid1

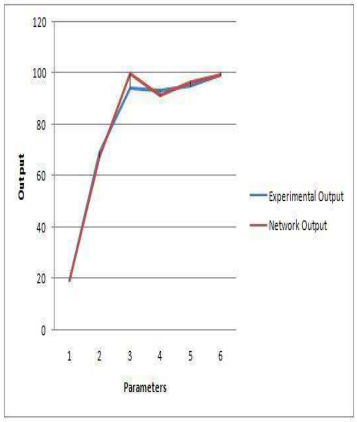

Figure s: Experimental and network output tanh

Table 9: Activation energy and thermodynamic parameters for adsorption of Fe^{+2} onto calcareous soil

E_a (kJ /mol)	ΔG^0 (kJ /mol)				ΔH^0 (kJ /mol)	ΔS^0 (J/mol)
	303 K	313 K	323 K	333 K		
9.47	-6.57	-6.72	-6.87	-7.01	-20.54	-0.015

3.13 ANN Model:

Three trained ANN models were tested and validated with the experimental results to estimate the Fe^{+2} concentrations. Finally in testing phase, the results showed that the network output is matched with experimental output (Figure q-s). Sigmoid1 model output curve is better fitted with the experimental data.

3.14 Cost Analysis:

Overall cost of the adsorbent material is governed by several factors which include its availability (whether it is natural, industrial/agricultural/domestic wastes or by-products or synthesized products), the processing required and reuse. Calcareous soil is available in abundance and collected from a

village of Birbhum district under soil (5ft from top soil) without any cost. Therefore the use of calcareous soil can be effectively utilized for removal of iron from drinking water.

4. Conclusion:

1) In this study, the adsorption ability of calcareous soil was investigated including operational parameters such as pH, adsorbent dose, stirring rate, contact time, initial Fe^{+2} concentrations, temperature and other co-ions.
2) The maximum adsorption of Fe^{+2} was 2.47 mg/g at 6.0 mg/L initial concentrations at pH 6.0.
3) Further, the adsorbent was characterized by FTIR, XRD, SEM techniques before and after adsorption which showed some significant changes.
4) The kinetic studies revealed that the adsorption process best fit the pseudo-second-order kinetic model and intraparticle diffusion was not the sole rate-limiting step.
5) The study on Langmuir isotherm model gave the best fit to the experimental data. The nature of adsorption of Fe^{+2} onto calcareous soil was physical as referred from the Dubinin-Radushkevich model as well as from E_a (activation energy) also.
6) The temperature strongly effects on the adsorption process and the maximum removal was observed at 303 K and the calculated thermodynamic parameters showed the spontaneous and exothermic nature of the adsorption.
7) According to ANN model sigmoid1 model is better fitted with the experimental results. The present study showed that calcareous soil could be used as a good and inexpensive adsorbent for practical application.

5. Acknowledgement:

The authors are grateful to Dr. Alak Kumar Ghosh, Associate Professor, Department of Chemistry, Burdwan University, Burdwan, West Bengal, India for recording FTIR data and they also extend their gratitude to Dr Srikanta Chakraborty, In charge of SEM, USIC, University of Burdwan, West Bengal, India for SEM study.

References:

1) Ahamad, K.U. and Jawed, M. (2011): Breakthrough column studies for iron (II) removal from water by wooden charcoal and sand: a low cost approach. *Int. J. Environ. Res.,* 5(1): 127-138.
2) Arivoli, S., Baskaran, P.K. and Venkatraman, B.R. (2011): Kinetics of adsorption of ferrous ion onto acid activated carbon from Zea Mays dust. *E-J.Chemistry.,* 8 (1): 185-195.
3) Atolaiye, B.O., Babalola, J.O., Adebayo, M.A. and Aremu, M.O. (2009): Equilibrium modeling and pH dependence of the adsorption capacity of *Vitex doniana* leaf for metal ions in aqueous solutions. *African J. Biotechnol.,* 8(3): 507-514.
4) Chowdhury, S. and Saha, P. (2010): Sea-shell powder as a new adsorbent to remove Basic Green4 (Malachite green) from aqueous solutions: Equilibrium, kinetic and thermodynamic studies. *Chem. Eng. J.,* 164: 168-177.
5) Dean, J.G., Bosqui, F,L. and Lanouette, K.H. (1972): Removing of heavy metals from waste water. *Environ. Sci. Technol.,* 6: 518-522.
6) Deviprasad, A.G. and Abdullah, M.A. (2009): Biosorption of Fe(II) from aqueous solution using Tamarind bark and potato peel waste : equilibrium and kinetic studies. *J. Applied Sc. Environ. Sanit.,* 4(3): 273-282.
7) Dogan, M., Alkan, M., Türkyılmaz, A. and Özdemir,Y. (2004): Kinetics and mechanism of removal of methylene blue by adsorption onto perlite. *J. Hazard. Mater.,* 109(B): 141-148.
8) Ellis, D., Bouchard, C. and Lantagne, G. (2000): Removal o f iron and manganese from groundwater by oxidation and microfiltration. *Desalination.,* 130: 255-264.
9) Freundlich, H. (1906): Over the adsorption in solution. *Z. Phys. Chem*., 57**(**A): 385.
10) Jordao, C.P., Fernandes, R.B.A., Ribeiro, K.L., Barros, P.M., Frontes, P.F. and PaulaSouza, F.M. (2010): a study on Al(III) and Fe(II) ions sorption by cattle manure vermicompost. *J. Wat. Air. Soil. Pollut.,* 210(1-4): 51-61.
11) Kalavathy, H., Karthik, B. and Miranda, L R. (2010): Removal and recovery of Ni and Zn from aqueous solution using activated carbon from *Hevea brasiliensis*: Batch and

column studies. *Colloid Surf B: Biointerf.,* 78: 291-302.

12) Karthikeyan, G. and Sivailango, S. (2008): Equilibrium sorption studies of Fe, Cu and Co ions in aqueous medium using activated Carbon prepared from *Ricinus communis Linn. J. Appli. Sci. Environ. Manag.,* 12(2): 81-87.

13) Kumar, P. S., Gayathri, R.and Arunkumar, R.P. (2010): Adsorption of Fe (II) ions from aqueous solution by Bengal gram husk powder: equilibrium isotherms and kinetic approach. *EJEAFChe*., 9 (6): 1047-1058.

14) Langmuir, I. (1916): The constitution and fundamental properties of solids and liquids. *J. Am. Chem. Soc*., 38: 2221.

15) Lu, H., Luan, M. and Zhang, J. (2009): A kinetic study on the Adsorption of Chromium (VI) onto a natural Material used as Landfill Liner. *EJGE*., 14: 1-10.

16) Mondal, M.K. (2010): Removal of Pb from aqueous solution by adsorption using activated tea waste. *Korean J. Chem. Eng.,* 27(1): 144-151.

17) Moreno, J. C., Gomez, R. and Giraldo, L. (2010): Removal of Mn, Fe, Ni and Cu ions from waste water using cow bone charcoal. *Materials.,* 3: 452-466.

18) Meenakhsipriya, B., Saravanan, K. and Sathiyavathi, S. (2009): Neural Based pH System in Effluent Treatment Process. *Modern Appl. Sci.,* 3(4): 166-176.

19) Najim,T.S., Elais, N.J. and Dawood, A.A. (2009): Adsorption of copper and Iron using low cost Materials as adsorbent. *E-J, Chemistry.,* 6 (1): 161-168.

20) Oladoja, N.A., Aboluwoye, C.O. and Oladimeji, Y.B. (2008): Kinetics and isotherm studies on methylene blue adsorption onto ground palm kernel coat. *Turk. J. Eng. Env. Sci.,* 32: 303-312.

21) Pandey, K. K., Prasad, G. and Singh, V. N. (1984): Removal of Cr(VI) from aqueous solution by adsorption on fly ash wollastonite. *J. Chem. Technol. Biotechnol*., 34(A): 367-374.

22) Renmin G., Yingzhi S., Jian C., Huijun L. and Chao Y. (2005): Effect of chemical modification on dye adsorption capacity of peanut hull. *Dyes and Pigments.,* 67: 179.

23) Saha, P., Chowdhury, S., Gupta, S. and Kumar, I. (2010): Insight into adsorption equilibrium, kinetics and thermodynamics of Malachite Green onto clayey soil of Indian Origin. *Chem. Eng. J*., 165(3): 874-882.

24) Sujana, M. G., Padhan, H. K. and Anand, S. (2009): Studies on sorption of some geomaterials for fluoride removal form aqueous solutions. *J. Hazard. Mater*., 161: 120-125.

25) Stewart, D., Yahiaoui, N., McDougall, G.J., Myton, K., Marque, C., Boudet, A.M. and Haigh, J. (1997): Fourier-transform infrared and Raman spectroscopic evidence for the incorporation of cinnamaldehydes into the lignin of transgenic tobacco (Nicotiana tabacum L.) plants with reduced expression of cinnamyl alcohol dehydrogenase. *Planta.,* 201: 311–318.

26) Tembhurkar, A. R. and Dongre, S. (2006): Studies on fluoride removal using adsorption process. *J. Environ. Sci. Eng.,* 48 (3): 151-156.

27) Theivarasu, C., Mylsamy, S. and Sivakumar, N. (2011): Cocoa shell as adsorbent for the removal of methylene blue from aquous solution: Kinetic and Equilibrium study. *Universal J. Environ. Res. Technol.,* 1: 70-78.

28) Vadivelan V. A. and Kumar K.V. (2005): Equilibrium, Kinetics, Mechanism, and Process design for the sorption of methylene blue onto rice husk. *J. Colloid. Interf. Sci.,* 286: 90-100.

29) Vaaramaa K. and Lehto J. (2003): Removal of metals and anions from drinking water by ion exchange. *Desalination.,* 155: 157.

30) Wasewar, K.L., Kumar, S. and Prasad B. (2009): Adsorption of Tin Using Granular Activated Carbon. *J. Environ. Protec. Sci.,* 3: 41-52.

31) Weber, W. J. and Morris, J. C. (1963): Kinetics of adsorption on carbon from solution. *J. Sanit. Eng. Div. Am. Soc. Civil. Eng.,* 89: 31.

32) World Health Organization (WHO), (1993): Guidelines for Drinking Water Quality, World Health Organization, Geneva. 1: 45-46.

33) Yeddou, N. and Bensmaili, A. (2007): Equilibrium and kinetic modeling of iron adsorption by eggshell in a batch system: effect of Temperature. *Desalination.,* 206: 127-134.